Submission code: PBPV7Q89BN

See this and other abstracts on our website: https://home.sbgf.org.br/Pages/resumos.php

Comparative Analysis of Seismic Inversion and Petroelastic Impedance Models in Marlim Sul Field, Campos Basin

ROSENBERG LIMA (PETROBRAS/UENF), FERNANDO MORAES (UENF)

Comparative Analysis of Seismic Inversion and Petroelastic Impedance Models in Marlim Sul Field, Campos Basin

Please, do not insert author names in your submission PDF file

Abstract

This study aims to compare acoustic impedance volumes derived from seismic inversion with those computed from petroelastic models based on petrophysical properties such as porosity, and oil, water, and gas saturations. The objective is to assess the discrepancies between the inverted and modeled impedances to calibrate the geological and flow simulation models. We intend to establish a metric to update the models and improve the inputs in a subsequent 4D seismic history-matching workflow. This methodology is applied in the Marlim Sul Field, Campos Basin.

Introduction

3D seismic data plays a fundamental role in building static reservoir models by enabling the integration of structural and property information beyond well locations. Since no single data type is sufficient, combining seismic data with logs, cores, and production data enhances model reliability. 4D seismic adds value by detecting pressure and saturation changes, helping to identify flow barriers and dynamic reservoir behavior. For effective integration, consistency between seismic data and geological models is crucial to avoid errors propagation during seismic history matching. Seismic attributes must be quantitatively linked to well data using statistical or machine learning techniques to predict petrophysical properties across the volume. These predictions reduce spatial uncertainty and support development planning. However, challenges remain—mainly due to differences in scale and resolution between seismic and geological data. Seismic vertical resolution (10–30 m) often fails to detect small-scale heterogeneities, unlike geological models based on well data. Additionally, seismic inversion is an inherently non-unique process, making it difficult to distinguish between similar lithologies. Integrating multiscale data remains complex but essential for building reliable reservoir models.

Dataset

The Marlim Sul Field is in the central portion of the Campos Basin, more than 120 km offshore, in water depths ranging from 800 to 2500 meters (ANP, 2021) (Figure 1). The field was discovered in 1987 and began production in 1994. The portion analyzed in this study corresponds to the central area of the field, as described by Ragagnin & Moraes (2008) (Figure 2), where Oligo-Miocene reservoirs are associated with a sand-rich submarine slope system. During the deposition of these sandstones, the Campos Basin displayed a physiography typical of a passive margin, with well-defined continental shelf, slope, and abyssal plain (De Gasperi & Catuneanu, 2014). Stratigraphically, the producing interval is subdivided into two zones: upper zone and lower zone (channel complex), which represent different sedimentation phases and production compartments. This study is based on an integrated dataset comprising well data, seismic data (acoustic impedance from inversion), geological interpretations, 3D geological and flow reservoir modeling, as well as laboratory experiments.

Methodology

To compare seismic inversion outputs with the petroelastic model, the original 3D acoustic impedance volume—provided in time domain—was first converted to depth using the associated 3D velocity cube. After that, a structural realignment between grids was required to ensure spatial consistency (depth-to-depth matching). Following structural alignment, lateral upscaling (horizontal resampling) was applied to match the 50 × 50 m horizontal resolution of the reservoir model.

Based on the geological/simulation model available, which includes petrophysical properties such as porosity, fluid saturations (oil, water, gas), shale volume and pore pressure, a petroelastic model was constructed. The saturated rock bulk modulus (Ksat) was calculated using Gassmann's equation (1951). Subsequently, seismic velocities (Vp, Vs), acoustic impedance (IP), shear impedance (IS), and Vp/Vs ratios were calculated. From petrogeophyscal studies IP was chosen as the most appropriate property to make comparison with inversion results.

After petroelastic modeling, IP must be constrained to the seismic scale for comparison with inversion results. It was also required a grid expansion with surrounding rock data to avoid null values. Seismic parameters are also assigned to inactive cells due to the importance of acoustic contrasts. Resampling is performed by averaging neighboring cells, and a smoothing filter is applied to simulate the limited seismic resolution (10–80 Hz). This process aligns the model with the practical frequency range of seismic data.

Results

After conditioning the acoustic impedance derived from seismic inversion (IPinv) with the model depths and conditioning of the petroelastic model with the seismic grid (IPpem), the data are ready for comparison (Figure 3). This comparison is primarily carried out using cross-plots between IPinv and IPpem volumes. An additional approach involves extracting average maps for the main production zones and comparing them through graphical analysis. Figure 4 presents a cross-plot of IPinv versus IPpem, color-coded by the percentage difference between the two datasets, with the 1:1 correlation line shown for reference. A correlation coefficient of 0.71 was obtained, indicating a strong relationship between the datasets.

Based on the cross-plot in Figure 4, the orthogonal deviation (i.e., the perpendicular distance of each point from the 1:1 correlation line) was calculated. As the percentage difference, this attribute serves as a measure of the similarity or mismatch between the datasets. Figure 5 shows the IPinv vs. IPpem cross-plot colored by orthogonal deviation.

From the IPinv and IPpem volumes, average maps were extracted for both datasets within the two producing zones of the field. Figure 6 displays the average maps of IPinv and IPpem for upper zone. Figure 7 shows the average maps for the lower zone, where an even stronger correlation is observed. These consistent correlations suggest that the geological and flow model is well-aligned with the seismic data, as represented by the acoustic impedance property derived from the inversion. In this case, a residual correction could be applied to geological model based on the restriction of these results.

Conclusions

Based on the cross-plot analysis and the results from the acoustic impedance maps derived from seismic inversion and the petroelastic model, this evaluation indicates that the 3D geological model and flow simulation are consistent with the variability observed in the seismic data. Therefore, the study is ready to be extended to 4D analysis, aiming for incorporation through seismic history matching.

Acknowledgments

The authors would like to express their gratitude to Petrobras for granting permission to publish this paper. They would also like to extend their appreciation to their colleagues Ana Clara Butelli

Fianco, Eurípedes Barsanulpho Luz Junior, Raunier Villain Fiuza, Tiago Tucci Maia and Caio Jean Matto Grosso da Silva.

References

AGÊNCIA NACIONAL DO PETRÓLEO, GÁS NATURAL E BIOCOMBUSTÍVEIS (ANP). *Plano de Desenvolvimento – Campo de Marlim Sul*. Rio de Janeiro: ANP, 2021. Disponível em: https://www.gov.br/anp/pt-br/assuntos/exploracao-e-producao-de-oleo-e-gas/desenvolvimento-e-producao/pd/marlim-sul.pdf.

De Gasperi, A., & Catuneanu, O. (2014). Sequence stratigraphy of the Eocene turbidite reservoirs in Albacora field, Campos Basin, offshore Brazil. *AAPG Bulletin*, *98*(2), 279‑313.

Gassmann, F., 1951. Elastic waves through a packing of spheres. *Geophysics*, **16**, p. 673‑685.

Ragagnin, G.M., Moraes, M.A.S. 2008. Seismic Geomorphology and Connectivity of Deepwater Reservoirs. SPE Reservoir Evaluation & Engineering. https://doi.org/10.2118/99852-PA.

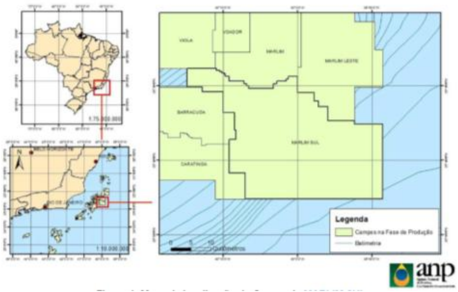

Figure 1: Location of Marlim Sul Field (extracted from ANP,2021).

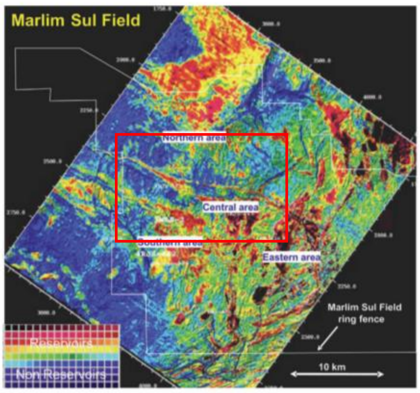

Figure 2: Location of central part of Marlim Sul Field (extracted from Ragagnin & Moraes, 2008).

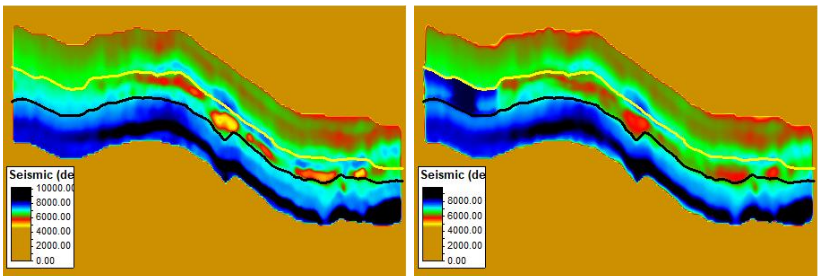

Figure 3: Example of Seismic section of IPinv x IPpem.

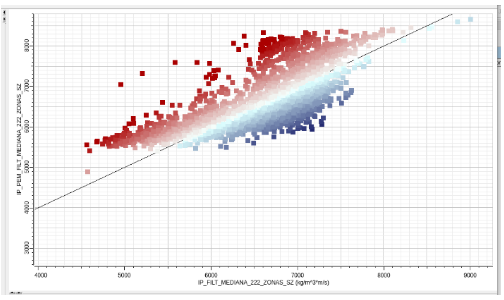

Figure 4: IPinv (from seismic inversion) x IPpem (from petroelastic model in seismic resample), colored by percentual difference (-20%:red and 20%:blue).

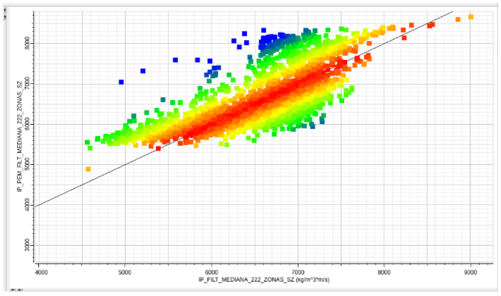

Figure 5: IPinv (from seismic inversion) x IPpem (from petroelastic model in seismic resample), colored by orthogonal deviation (0 to 2000).

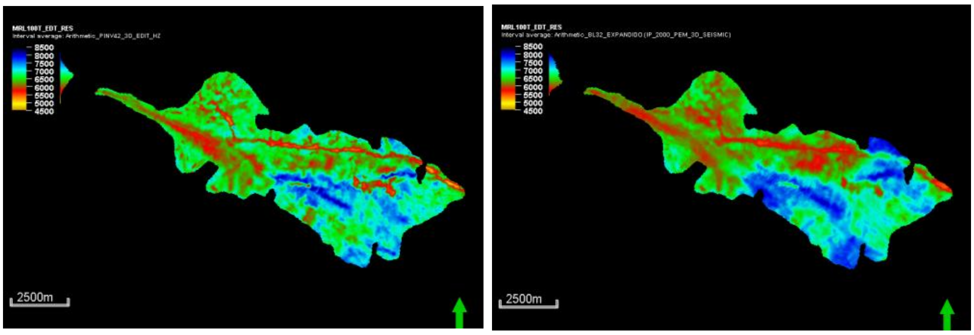

Figure 6: Acoustic impedance maps (IPinv and IPpem) from the upper zone of Marlim Sul Field.

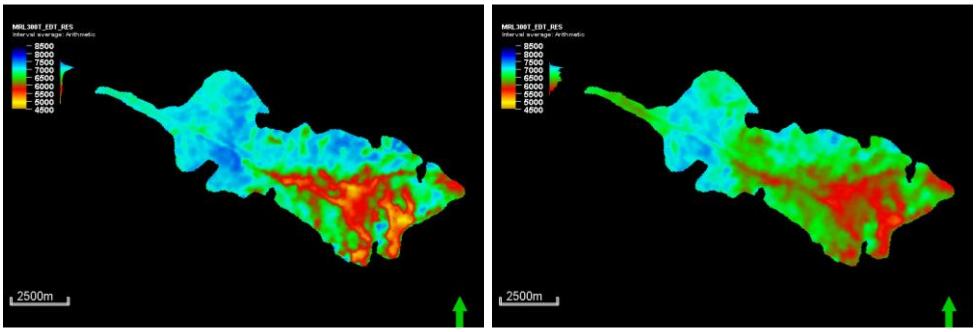

Figure 7: Acoustic impedance maps (IPinv and IPpem) from the lower zone of Marlim Sul Field.